Lawrence Berkeley National Laboratory

Lawrence Berkeley National Laboratory

Title

SURFACE RECONSTRUCTION AND CHEMICAL EVOLUTION OF STOICHIOMETRIC LAYERED CATHODE MATERIALS FOR LITHIUM-ION BATTERIES

Permalink

https://escholarship.org/uc/item/44q1n09z

Author

Lin, Feng

Publication Date

2014-09-01

eScholarship.org Powered by the California Digital Library
University of California

This document was prepared as an account of work sponsored by the United States Government. While this document is believed to contain correct information, neither the United States Government nor any agency thereof, nor the Regents of the University of California, nor any of their employees, makes any warranty, express or implied, or assumes any legal responsibility for the accuracy, completeness, or usefulness of any information, apparatus, product, or process disclosed, or represents that its use would not infringe privately owned rights. Reference herein to any specific commercial product, process, or service by its trade name, trademark, manufacturer, or otherwise, does not necessarily constitute or imply its endorsement, recommendation, or favoring by the United States Government or any agency thereof, or the Regents of the University of California. The views and opinions of authors expressed herein do not necessarily state or reflect those of the United States Government or any agency thereof or the Regents of the University of California.

SURFACE RECONSTRUCTION AND CHEMICAL EVOLUTION OF STOICHIOMETRIC LAYERED CATHODE MATERIALS FOR LITHIUM-ION BATTERIES

Feng Lin,[1] Isaac M. Markus,[1,2] Dennis Nordlund,[3] Tsu-Chien Weng,[3] Mark D. Asta,[2] Huolin L. Xin,[4] and Marca M. Doeff[1]*

1. Environmental Energy Technologies Division, Lawrence Berkeley National Laboratory, Berkeley, CA 94720, USA
2. Department of Materials Science and Engineering, University of California, Berkeley, CA 94720, USA
3. Stanford Synchrotron Radiation Lightsource, SLAC National Accelerator Laboratory, Menlo Park, CA 94025, USA
4. Center for Functional Nanomaterials, Brookhaven National Laboratory, Upton, NY 11973, USA

* Feng Lin: flin@lbl.gov

Introduction

Stoichiometric $LiNi_xMn_xCo_{1-2x}O_2$ (NMC) represents a family of prominent cathode materials with potential to improve energy densities, reduce costs and enhance safety for plug-in hybrid electric vehicles (PHEVs) and electric vehicles (EVs). The challenge of achieving these goals is attributed to undesirable modifications of $LiNi_xMn_xCo_{1-2x}O_2$ materials during high-voltage cycling, which leads to gradual buildup of cell impedance and simultaneous capacity fading. The purpose of this study was to correlate surface and bulk structural characteristics of $LiNi_xMn_xCo_{1-2x}O_2$ (NMC, **Figure 1**) materials with the electrochemical performance. Aided with the state-of-the-art atomic-scale annular dark-field scanning transmission electron microscopy (ADF/STEM) and electron energy loss spectroscopy (EELS) as well as ensemble-averaged synchrotron X-ray absorption spectroscopy, the present study provides insights into the surface reconstruction and chemical evolution in NMC materials and directly correlates with the origin(s) of long-standing challenges in NMC materials, including high-voltage capacity fading, impedance buildup and first-cycle coulombic inefficiency. Note that the surface reconstruction and chemical evolution herein refer to the formations of surface reduced layer (R-3m to Fm-3m transition) and surface reaction layer (SRL), respectively. Our results represent an important pathway towards understanding layered cathode materials and the methodology herein provides guidance to advance knowledge for battery materials in general.

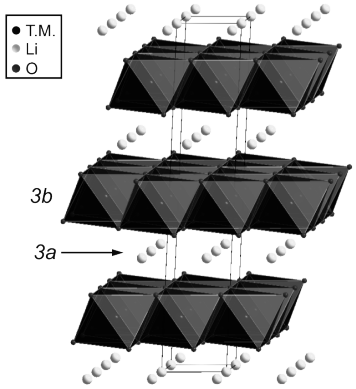

Figure 1. Schematic representation for the layered structure of NMC materials with *c*-axis oriented vertically: Li *3a* site and TM *3b* site.

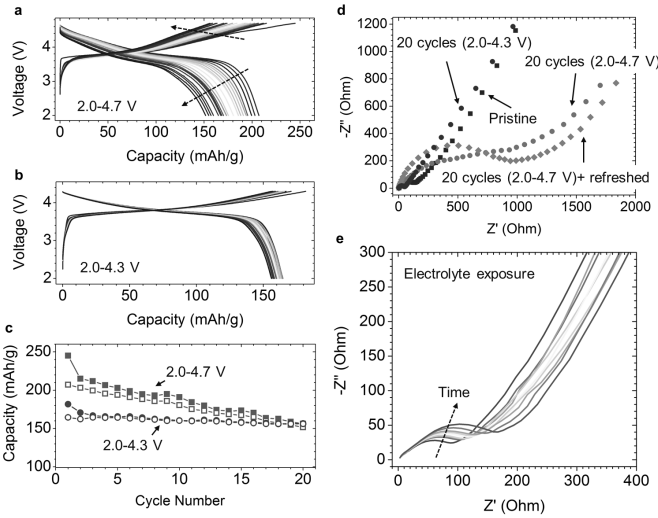

Figure 2. (a) Charge-discharge profiles at 2.0-4.7 V for 20 cycles at C/20. (b) Charge-discharge profiles at 2.0-4.3 V for 20 cycles at C/20. (c) Charge and discharge capacities as functions of cycle number at 2.0-4.7 V and 2.0-4.3 V respectively. (d) Nyquist plots of impedance data (e) A series of Nyquist plots for a pristine NMC electrode exposed to electrolytic solution for various periods up to 7 days.

Experimental

$LiNi_{0.4}Mn_{0.4}Co_{0.18}Ti_{0.02}O_2$ materials were synthesized using a co-precipitation method. For the synthesis of $LiNi_{0.4}Mn_{0.4}Co_{0.18}Ti_{0.02}O_2$, 250 mL of an aqueous solution of transition metal nitrates (0.16 M $Ni(NO_3)_2$, 0.16 M $Mn(NO_3)_2$, 0.072 M $Co(NO_3)_2$), 0.008 M $TiO(SO_4)\cdot xH_2O$ and 250 mL of 0.8 M LiOH aqueous solution were dripped simultaneously into a beaker using a Masterflex C/L peristaltic pump and stirred continuously. The precipitate was collected, filtered and washed with DI water, and then dried overnight at 100 ºC in the oven. The dried precipitate was ball-milled with LiOH and then heated in air at 900 ºC for 3 h with a ramp of 2 ºC/min.

Composite electrodes were prepared with 84 wt% active material, 8 wt% polyvinylidene fluoride, 4 wt% acetylene carbon black and 4wt% SFG-6 synthetic graphite in N-methyl-2-pyrrolidinone and cast onto carbon-coated aluminum current collectors with typical active material loadings of 6-7 mg/cm^2. 2032-type coin cells were assembled in a helium-filled glove box using the composite electrode as the positive electrode and Li metal as the negative electrode. A Celgard 2400 separator and 1 M $LiPF_6$ electrolyte solution in 1:2 w/w ethylene carbonate/dimethyl carbonate were used to fabricate the coin cells. Battery testing was performed on a computer controlled VMP3 potentiostat/galvanostat (BioLogic).

X-ray Diffraction (XRD) on powder samples was performed on a Bruker D2 Phaser diffractometer using CuKα radiation. Scanning electron microscopy (SEM) was performed on a JEOL JSM-7000F. XAS measurements were performed on the 31-pole wiggler beamline 10-1 at Stanford Synchrotron Radiation Lightsource (SSRL) using a ring current of 350 mA and a 1000 l·mm^{-1} spherical grating monochromator with 20 μm entrance and exit slits, providing ~1011 ph·s^{-1} at 0.2 eV resolution in a 1 mm^2 beam spot. During the measurements, all battery electrode samples were attached to an aluminum sample holder using conductive carbon. XAS signals were collected at several positions on individual electrodes to ensure that data was representative of the sample. A 200 keV and 300 keV

probe-corrected field-emission scanning/transmission electron microscopes (S/TEM) were used for annular dark-field STEM (ADF-STEM) imaging and spatially resolved electron energy loss spectroscopy (EELS). Spectroscopic imaging was performed with an Enfina spectrometer on a Hitachi 2700C dedicated STEM.

Results and Discussion

As shown in **Figure 2**, in lithium-metal half-cells, capacity fading and impedance buildup are more pronounced at high-voltage cycling (2.0-4.7 V *vs.* Li^+/Li). The degradation of battery electrodes is completely irreversible, namely, after high-voltage cycles, refreshing electrolyte or switching to low-voltage cycling could not recover the performance (date not shown). Impedance buildup was also observed when exposed to electrolyte for an extended period (**Figure 2e**).

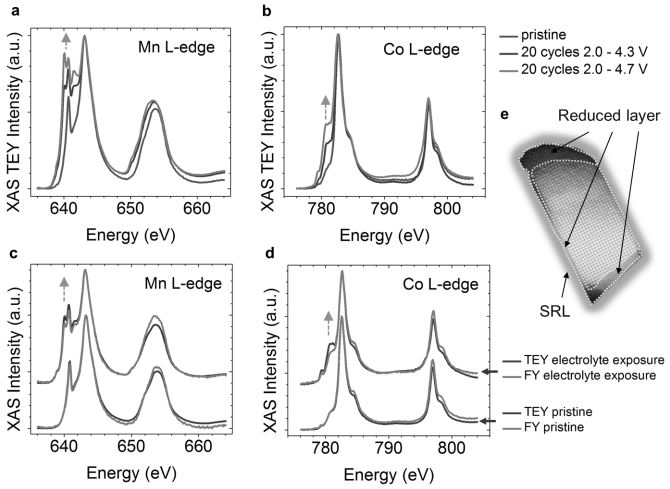

Figure 3. Effects of cycling voltages and electrolyte exposure. (a) Mn L-edge XAS/TEY spectra and (b) Co L-edge XAS/TEY spectra of pristine and cycled electrodes (20 cycles). (c) Mn L-edge XAS/TEY/FY spectra and (d) Co L-edge XAS/TEY/FY spectra of a pristine electrode and one exposed to electrolytic solution for 7 days. The dashed arrows in (a-d) indicate the increase of transition metals having low oxidation states. (e) Schematic illustration of reduced layer and SRL.

Here we show that the surface reduced layer (surface reconstruction) is related to the inferior capacity retention observed under high-voltage cycling conditions. As shown in **Figures 3a** and **3b**, a reduced layer gradually forms at the top few nanometers after extended high-voltage cycles. The contribution of low-valence transition metals to XAS signal is more significant after high-voltage cycling (indicated by dashed arrows). DFT calculation showed that, under oxygen partial pressure ranging from 10^{-12} atm to 1 atm, after about 60% of lithium has been removed from the NMC structure, it becomes favorable to form the rock salt structure (data not shown). Previous reports have attributed the surface reduced layer mainly to electrochemical processes with little attention dedicated to the effects of electrode-electrolyte reactivity. Here we showed that a surface reduced layer similar to the ones observed during high-voltage cycling is also created after an NMC electrode was immersed in the electrolyte (**Figures 3c** and **3d**), although it is thinner.

As shown in **Figure 4**, the slightly mismatched lattices between Fm-3m {111} and R-3m {003} allow for the epitaxial growth of (Ni, Mn, Co)O on the NMC layered structure. Furthermore, we observed that the growth of rock-salt structure on NMC structure showed an anisotropic characteristic (data not shown).

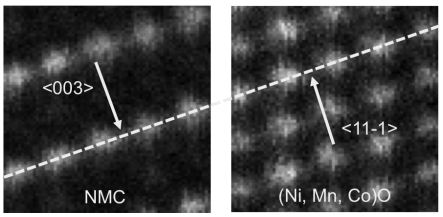

Figure 4. Lattice match-up between NMC layered structure and rock-salt (Ni, Mn, Co)O structure.

This study has enabled the following understanding: (1) layered/R-3m to rock-salt/Fm-3m transition and reaction layer (data not shown) at the surfaces lead to the high-voltage instability of NMC materials; (2) surface reconstruction predominantly occurs along the lithium diffusion channels, *i.e.*, facet-dependent; (3) The study suggests an orientation-specific surface functionalization for enhanced battery performance. Several important phenomena would have been omitted without such a study at complementary length scales (XAS in combination with STEM-EELS). Finally, this work sets a refined example for the study of surface reconstruction and chemical evolution in battery materials using combined diagnostic tools at complementary length scales. More information about this work could be found in *Nat. Commun.* **2014**, *5*, 3529 DOI: 10.1038/ncomms4529.

Acknowledgment

This work was supported by the Assistant Secretary for EERE, Office of Vehicle Technologies of the U.S. Department of Energy under Contract No. DE-AC02-05CH11231 under the BATT Program. The synchrotron XAS was carried out at the Stanford Synchrotron Radiation Lightsource, a Directorate of SLAC National Accelerator Laboratory and an Office of Science User Facility operated for the U.S. Department of Energy Office of Science by Stanford University. S/TEM and EELS experiments were performed at the Center for Functional Nanomaterials (BNL), which is supported by the U.S. Department of Energy, Office of Basic Energy Sciences under Contract No. DE-AC02-98CH10886, and at National Center for Electron Microscopy (LBNL), which is supported by the U.S. Department of Energy (DOE) under Contract No. DE-AC02-05CH11231. This work made use of computational resources provided by the National Energy Research Supercomputer Center (NERSC), which is supported by the Office of Science of the US Department of Energy under Contract DE-AC03-76SF00098 and the Extreme Science and Engineering Discovery Environment (XSEDE), which is supported by National Science Foundation grant number OCI-1053575. I.M.M acknowledges the support of the NSF graduate research fellowship program. H.L.X conducted a portion of the TEM work when he was a postdoctoral fellow in Dr. Haimei Zheng's group at LBNL and thanks Dr. Haimei Zheng for her support.

References

1. Kam, K. C.; Doeff, M. M. *J. Mater. Chem.* **2011**, *21*, 9991.
2. Kam, K. C.; Mehta, A.; Heron, J. T.; Doeff, M. M. *J. Electrochem. Soc.* **2012**, *159*, A1383–A1392.
3. Lin, F.; Markus, I. M.; Nordlund, D.; Weng, T.-C.; Xin, H. L.; Doeff, M. M. *Nat. Commun.* **2014**, *5*, 3529 DOI: 10.1038/ncomms4529.
4. Xu, B.; Fell, C. R.; Chi, M.; Meng, Y. S. *Energy Environ. Sci.* **2011**, *4*, 2223.